Biochemistry

 Volume 36, Number 40 October 7, 1997

*Accelerated Publications*

# Pulsed EPR Structure Analysis of Photosystem I Single Crystals: Localization of the Phylloquinone Acceptor†

Robert Bittl,* Stephan G. Zech, Petra Fromme, Horst T. Witt, and Wolfgang Lubitz

*Max-Volmer-Institut für Biophysikalische Chemie und Biochemie, Technische Universität Berlin, Strasse des 17. Juni 135, 10623 Berlin, Germany*

*Received July 9, 1997; Revised Manuscript Received August 18, 1997*⊗

ABSTRACT: A novel application of electron paramagnetic resonance (EPR) is reported to gain three dimensional structural information on cofactors in proteins. The method is applied here to determine the unknown position of the electron acceptor $Q_K$, a phylloquinone (vitamin $K_1$), in the electron transfer chain in photosystem I of oxygenic photosynthesis. The unusual electron spin echo (out-of-phase echo) observed for the light induced radical pair $P_{700}^{\bullet+}Q_K^{\bullet-}$ in PS I allows the measurement of the dipolar coupling between the two radical pair spins which yields directly the distance between these two radicals. Full advantage of the information in the out-of-phase echo modulation can be taken if measurements using single crystals are performed. With such samples, the orientation of the principal axis of the dipolar interaction, i.e., the axis connecting $P_{700}^{\bullet+}$ and $Q_K^{\bullet-}$, can be determined with respect to the crystal axes system. An angle of $\theta = (27 \pm 5)°$ between the dipolar coupling axis and the crystallographic *c*-axis has been derived from the modulation of the out-of-phase echo. Furthermore, the projection of the dipolar axis onto the crystallographic *a*,*b*-plane, is found to be parallel to the *a*-axis. The results allow for the determination of two possible locations of $Q_K$ within the electron transfer chain of photosystem I. These two positions are related to each other by the pseudo $C_2$ symmetry of the chlorophyll cofactors.

The primary photoreaction in photosystem I (PS I) is a transmembrane electron transfer from a chlorophyll *a* dimer, $P_{700}$, via intermediary electron carriers to an 4Fe-4S iron sulfur cluster (for a review see ref 1). A 4 Å resolution model of PS I has been derived from single crystal X-ray structure analysis (*2*). Six chlorophyll *a* molecules and three 4Fe-4S clusters have been assigned to the electron transport chain. The chlorophyll molecules are arranged in two branches which are related by an approximate $C_2$ symmetry. However, the quinone acceptor $Q_K$ (previously called $A_1$) forming the link between the chlorophyll *a* carriers and the 4Fe-4S clusters has not yet been located. Here we report pulsed EPR experiments performed on the light-induced radical pair state $P_{700}^{\bullet+}Q_K^{\bullet-}$ in PS I single crystals as a function of the crystal orientation. From these experiments, the magnitude and orientation dependence of the dipolar spin−spin interaction can be determined. This yields the vector connecting the two partners of the radical pair within the crystal axes system. With the known position of $P_{700}$,

† This study was supported by Deutsche Forschungsgemeinschaft (Sfb 312 TP A3, A4), Fonds der Chemischen Industrie (to H.T.W. and W.L.), and a NaFöG Berlin fellowship (to S.G.Z.).

* Corresponding author fax: +49-30-314-21-122. E-mail: bittl@pair.chem.TU-Berlin.DE.

⊗ Abstract published in *Advance ACS Abstracts,* September 15, 1997.

[1] Abbreviations: $A_0$, primary electron acceptor; *D*, dipolar coupling constant; $eC_n$, electron carrier; ENDOR, electron nuclear double resonance; EPR, electron paramagnetic resonance; ESE, electron spin echo; ESEEM electron spin echo envelope modulation; $F_X$, $F_{A/B}$, iron sulfur clusters; *J*, isotropic exchange coupling; $P_{700}$, primary electron donor; PS I, photosystem I; $Q_K$, phylloquinone electron acceptor; SFT, sine Fourier transform.

S0006-2960(97)01645-0 CCC: $14.00 

the position of the acceptor $Q_K$ in the structural model of the electron transfer chain in PS I can be deduced. This method should be generally applicable to transient radical pair states in other proteins, e.g., photolyase (*3*) and coenzyme $B_{12}$ dependent enzymes (*4*).

The principle of the experiment is based on photoexcitation of the primary donor $P_{700}$ followed by rapid electron transfer from $P_{700}^*$ yielding the spin polarized radical pair state $P_{700}^{\bullet+}Q_K^{\bullet-}$. After the light excitation, the amplitude of the electron spin echo (ESE) at time $\tau$ following a $(\zeta/2) - \tau - \zeta$ microwave pulse sequence with flip angle $\zeta \approx 130°$ is recorded as a function of $\tau$. Due to the particular population of the energy levels of the radical pair, the echo signal is shifted from absorption to dispersion (out-of-phase) (*5*). The echo amplitude exhibits an oscillatory behavior as a function of $\tau$. The oscillation frequency depends on the spin−spin interaction between the two radicals (*5*). The two contributions to the spin−spin interaction, dipolar, and exchange coupling can be separated (*6*−*9*). The dipolar interaction exhibits a simple distance and orientation dependence and, thus, can be easily used to derive structural information.

From an unoriented sample, e.g., frozen solution, the principal value of the dipolar interaction can be obtained. This principal value yields one dimensional structural information, i.e., the distance between the unpaired electron spins. Recently, this method has been used by two groups to determine the distance $r$ between $P_{700}^{\bullet+}$ and $Q_K^{\bullet-}$ in PS I (*7*−*9*). The data are in excellent agreement, with $r = 25.4 \pm 0.3$ Å obtained by our group (*7*, *8*) and $r = 25.3 \pm 0.3$ Å by Dzuba *et al.* (*9*).

In addition, measurements on oriented samples such as single crystals also allow a determination of the orientation of the dipolar axis, i.e., the axis connecting the two unpaired electron spins, within the crystal axes system. Therefore, if the location of one of the two species carrying the unpaired spins is known, the postition of the other can be determined. This possibility of obtaining three dimensional structural information on cofactors in proteins has not been exploited so far. The method is complementary to other techniques for structure determination and can help, e.g., in the assignment of electron densities in X-ray crystallographic maps.

## MATERIALS AND METHODS

Crystals of PS I from *Synechococcus elongatus* were prepared as previously described (*2*). These crystals belong to the hexagonal space group $P6_3$ with two trimers of PS I in the unit cell. The crystallographic 3-fold axis is parallel to the long needle axis of the crystals. For the EPR measurements the crystals were incubated in a buffer containing 1.5 M sucrose as a cryoprotectant and 10 mM sodium ascorbate to keep $P_{700}$ reduced. The incubated crystals were mounted on a quartz rod in a trough perpendicular to the long axis of the rod. Most of the solution surrounding the crystals was removed, and the crystals were frozen rapidly in liquid nitrogen. The frozen crystals in the quartz rod were then transfered into the helium cooled EPR probehead. The time-resolved EPR setup has been described elsewhere (*8*).

## RESULTS AND DISCUSSION

The information on the spin−spin interaction contained in the modulation of the out-of-phase echo can be best visualized by a sine Fourier transform (SFT) of the time signals. Figure 1 shows the SFT of the echo modulation for $P_{700}^{\bullet+}$ $Q_K^{\bullet-}$ for rotation of the PS I crystal perpendicular to the *c*-axis. The angle between the external magnetic field and the needle axis is given by $\alpha$. The top trace is obtained from an unoriented frozen PS I solution. The single crystal rotation pattern exhibits the expected 180° periodicity and, additionally, a mirror symmetry consistent with the assumed coincidence of the 3-fold crystallographic axis with the long axis of the crystal. At the rotation angle corresponding to the mirror symmetry axis ($\alpha = 90°$ in Figure 1), the external magnetic field $B_0$ is aligned perpendicular to the crystallographic 3-fold axis, i.e., in the crystallographic *a*,*b*-plane. Rotation of the crystal by 90° ($\alpha = 0°$ and 180°) places the magnetic field $B_0$ parallel to the crystallographic 3-fold axis with all six PS I complexes in the unit cell being magnetically equivalent. The equivalence of all six PS I complexes for this orientation is best observed for the cw-EPR signal of the iron-sulfur cluster $F_A$ (*10*, *11*). We therefore recorded this signal to assure the correct alignment of the crystal (data not shown).

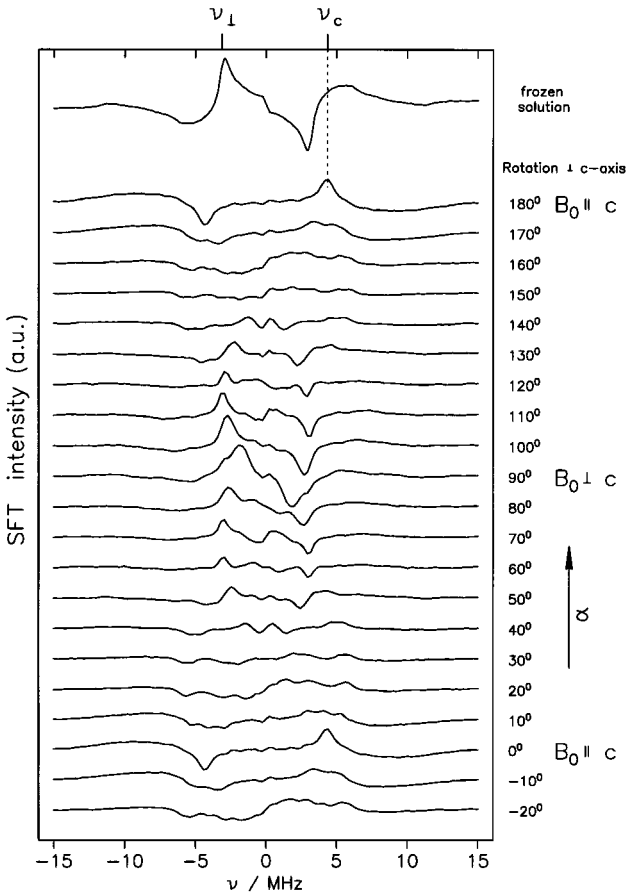


FIGURE 1: Sine-Fourier transforms of the echo modulation of the radical pair $P_{700}^{\bullet+}Q_K^{\bullet-}$ in PS I. The top trace is for a frozen PS I solution. The other traces show the angular dependence of the spectra for a rotation of a PS I single crystal perpendicular to the needle axis. At angles $\alpha = 0°$ and $\alpha = 180°$, the external magnetic field $B_0$ is aligned parallel to the needle axis which coincides with the crystallographic *c*-axis. The frequency $\nu_\perp$ arises from those PS I complexes with the dipolar axis perpendicular to $B_0$. For the single crystal with the *c*-axis aligned parallel the $B_0$ the frequency $\nu_c$ is observed.

The most intense feature in the trace for the frozen solution at $\nu_\perp \approx +3.1$ MHz arises from those PS I complexes with the $P_{700}^{\bullet+}-Q_K^{\bullet-}$ axis perpendicular to the external magnetic

field $B_0$. The frequency $\nu_\perp$ contains the distance information. In the orientation−dependent single crystal spectra, important features are the signal extrema at $\nu_c = \pm 4.4$ MHz for the two orientations with $B_0 \parallel \nu(\alpha = 0°$ and 180°). Insertion of the values for $D$, $J$, and $\nu_c$ into the equation for the angular dependence of the dipolar interaction immediately yields the angle $\theta$ between the $P_{700}^{\bullet+}-Q_K^{\bullet-}$ axis and the crystallographic $c$-axis. With $|\nu_c| = |2J - 2D(\cos^2\theta - 1/3)|$ and $D = -170$ $\mu$T, $J = 1$ $\mu$T as determined from the frozen solution experiments (*7*, *8*) we obtain $\theta = (27 \pm 5)°$. A large fraction of the error margin results from the remaining uncertainty in the alignment of the crystal with respect to the external magnetic field.

The determined angle $\theta$ and the $P_{700}^{\bullet+}-Q_K^{\bullet-}$ distance $r$ given above define a circle of possible $Q_K$ locations in a plane parallel to the crystallographic *a*,*b*-plane and a midpoint in the center of the unpaired spin density of $P_{700}^{\bullet+}$. Electron nuclear double resonance (ENDOR) experiments on $P_{700}^{\bullet+}$ in PS I single crystals (*12*, *13*) have shown that the unpaired spin is located almost exclusively on one Chl *a* of $P_{700}^{\bullet+}$. However, it is not known which of the two Chl *a* molecules carries the unpaired spin. Of the two posibilities we consider first that the spin on $P_{700}^{\bullet+}$ is centered on the Chl *a* molecule labeled $eC_1'$ in the structural model of PS I.

A projection of the resulting circle of possible $Q_K^{\bullet-}$ locations is shown in Figure 2 (top) together with the electron transfer components of PS I located by X-ray crystallography (*2*). The view direction is parallel to the membrane (*a*,*b*) plane and along the Mg−Mg line connecting the two Chl *a* species, $eC_1$ and $eC_1'$, forming $P_{700}$. The plane of the circle has a distance of 22.6 ± 1 Å from $P_{700}$ and a distance of 9.4 ± 1 Å from the first iron sulfur cluster $F_X$. The circle radius is 11.5 ± 2 Å.

To provide information on the location of $Q_K$ in the crystallographic *a*,*b*-plane, we have analyzed the spectrum at $\alpha = 90°$ in Figure 1. At this crystal orientation, the field $B_o$ is perpendicular to the *c*-axis, i.e., it lies in the *a*,*b*-plane. The crystal was mounted such that, for this orientation, $B_o$ was also perpendicular to a macroscopic plane of the crystal. From the shoulder at $|\nu_1| = 3.1$ MHz and the peak at $|\nu_2| = 1.7$ MHz in the SFT, with an intensity ratio of approximately 1:2, the angle $\phi$ between $B_o$ and the projection of the $P_{700}^{\bullet+}-Q_K^{\bullet-}$ dipolar axis onto the *a*,*b*-plane can be derived. For two PS I centers of the six in the unit cell, $\phi_1 = 90 \pm 10°$, and for the remaining four, PS I $\phi_2 = 30 \pm 10°$ is obtained. Assuming that the macroscopic planes are crystallographic *a*,*c*-planes (or crystallographically equivalent planes), it follows furthermore that the projection of the $P_{700}^{\bullet+}-Q_K^{\bullet-}$ axis onto the *a*,*b*-plane must be parallel to the *a*-axis (or an equivalent axis). Six orientations of the $P_{700}^{\bullet+}-Q_K^{\bullet-}$ axis in a PS I monomer are, therefore, possible due to the 6-fold symmetry of the space group. The six possible positions of $Q_K$ are depicted in Figure 2 (bottom) in a projection onto the *a*,*b*-plane considering the unpaired spin of $P_{700}^{\bullet+}$ located on $eC_1'$. The $Q_K$ position 1 is in this projection almost superimposed on the monomeric Chl *a* electron carrier $eC_3$.

The six different $Q_K$ positions can be distinguished on the basis of independent arguments. The beginning of a highly conserved LxSzRGYWQELIE sequence of residues in PsaA and PsaB (*14*) is found at the connection between helices *m*′ and *n*′ (*m* and *n*) (*2*). This conserved sequence has been suggested to be the $Q_K$ binding site (*15*). Position 1 in Figure 2 (bottom) is close to the connection between helices *m*′ and *n*′ in the 4 Å model of PS I (*2*). Therefore, we assign the most likely $Q_K$ location to position 1. This is the position with the shortest distance between the spectroscopically identified first electron acceptor $A_0$ [$eC_3$ or $eC_3'$ (*2*)] and $Q_K$ with a $Q_K$ (center-to-center) distance to $eC_3$ of 7.5 ± 2 Å. In positions 3 and 4, this distance is 11 ± 2 Å and in positions 2, 5, and 6 it is 13−16 Å. The center-to-center distance between the $Q_K$ position 1 and $eC_3$ of 7.5 ± 2 Å is similar to the 7−8 Å edge-to-edge distance between $A_0$ and $Q_K$ estimated from the electron transfer rate (*16*). Thus, the location of $Q_K$ can be characterized by the following

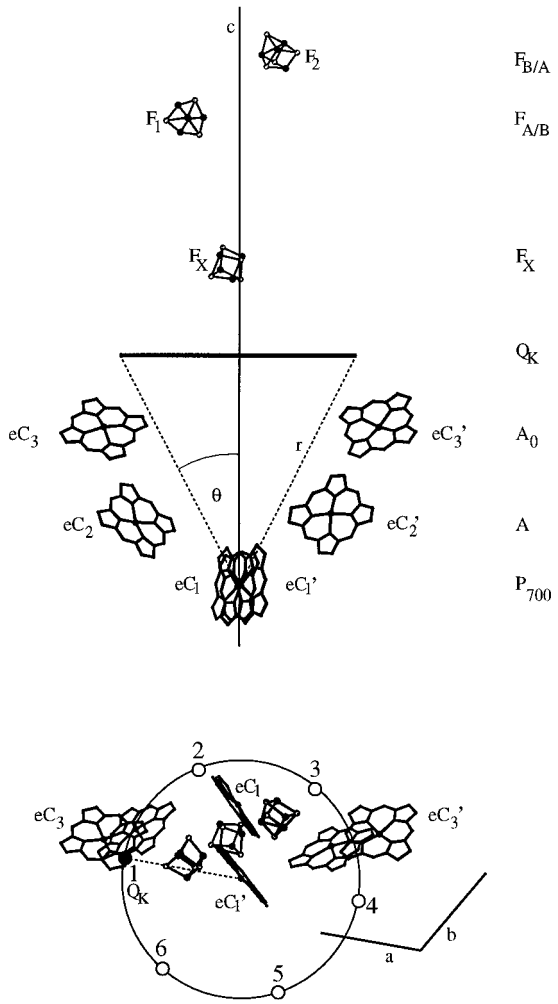


FIGURE 2: Location of the members of the electron transport chain in PS I as determined by X-ray crystallography and the possible positions of the phylloquinone $Q_K$ deduced from the EPR data presented here. It should be noted that two phylloquinone molecules are present in PS I per $P_{700}$. The view direction in the top part is parallel to the *a*,*b*-plane and along the Mg−Mg axis between the two Chl *a* molecules $eC_1$ and $eC_1'$ assigned to the primary donor $P_{700}$. The *c*-axis is parallel to the crystallographic $C_3$-axis. The thick horizontal line is a side view of the circle of possible $Q_K$ locations defined by the angle $\theta = 27°$ between the *c* axis and the connection line between $P_{700}^{\bullet+}$ and $Q_K^{\bullet-}$ together with the $P_{700}^{\bullet+}-Q_K^{\bullet-}$ distance $r$ = 25.4 Å. The bottom part shows a projecton of the electron transfer chain onto the crystallographic *a*,*b*-plane. The *a*,*b*-axes are parallel to the respective crystallographic axes. The unpaired spin density on $P_{700}^{\bullet+}$ is assumed to be centered on $eC_1'$. The six numbered points indicate the $Q_K$ positions on the ring defined above and with an angle $\phi = 0°$ between the projection of the $P_{700}^{\bullet+}-Q_K^{\bullet-}$ axis (dashed line for position 1) and the *a* (or an equivalent) axis. Position 1 (filled point) has the shortest distance to the monomeric Chl *a* $eC_3$.

structural parameters:

distance $eC_1'-Q_K = 25.4 \pm 0.3$ Å,
angle $\angle (eC_1'-Q_K, c) = 27° \pm 5°$

distance $eC_3-Q_K = 7.5 \pm 2$ Å,
and distance $F_X-Q_K = 14 \pm 2$ Å

The location of $Q_K$ given here is in disagreement with the position of $Q_K$ suggested recently on the basis of the relaxation properties of the electron transfer components in PS I (*17*). There, a $F_X-Q_K$ distance of 20−30 Å has been deduced. However, this distance determination depends on several parameters which have only been estimated. It should be noted that neither of the five other positions consistent with our EPR data but ruled out on the basis of independent arguments shows a $F_X-Q_K$ distance in the 20−30 Å range. In contrast to the discrepancy with the data of ref 17, the $F_X-Q_K$ distance given above is in good agreement with a recent estimate of 14.2 Å (*18*) based on measurements of the orientation of $Q_K^{\bullet-}$. The $14 \pm 2$ Å $F_X-Q_K$ center-to-center distance is also in qualitative agreement with the 7−11 Å edge-to-edge distance deduced form the $Q_K^{\bullet-}$ to $F_X$ electron transfer rate (*19*, *20*).

So far we have assumed that the unpaired spin density of $P_{700}^{\bullet+}$ is localized on $eC_1'$. With the unpaired spin density of $P_{700}^{\bullet+}$ centered on $eC_1$ we obtain an alternative location for $Q_K$. This position (not shown) is related to the one described above by a $C_2$ symmetry operation with the symmetry axis parallel to the crystallographic *c*-axis and centered in the mid point of the Mg−Mg axis between $eC_1$ and $eC_1'$. This symmetry axis is to a good approximation the local pseudo $C_2$ symmetry axis of the chlorophyll species $eC_n$. Therefore, the alternative $Q_K$ position is then superimposed on $eC_3'$ in the projection onto the membrane plane in a similar way than before on $eC_3$. The structural parameters for this site are identical (after replacing $eC_1'$ by $eC_1$ and $eC_3$ by $eC_3'$) to the ones given above except for the $F_X-Q_K$ distance. Since $F_X$ is displaced from the axis connecting the centers of $eC_1$ and $eC_1'$ in Figure 2 (bottom), a slightly longer $F_X-Q_K$ distance is obtained for the second position. However, the difference between the two $F_X-Q_K$ distances is not significant and can, therefore, at present not be used to distinguish between the two $Q_K$ positions. Which, of the two alternative positions for $Q_K$, corresponds to the reduced phylloquinone in the electron transfer pathway stays undetermined because it is not yet known which of the two halfes of the oxidized $P_{700}$ carries the unpaired spin density.

The location for $Q_K$ obtained here correspond to an electron density in an improved 4 Å resolution map of PS I (*21*).

## ACKNOWLEDGMENT

We thank A. Kamlowski and D. Stehlik (FU Berlin) for collaborating in transient and cw-EPR experiments on PS I single crystals and valuable discussions. The picture of the arrangement of the electron transfer chain as determined by X-ray crystallography on which Figure 2 is based was kindly provided by W.-D. Schubert (FU Berlin) whom we also thank for helpful discussions.

## REFERENCES

1. Brettel, K. (1997) *Biochim. Biophys. Acta 1318*, 322−373.
2. Krauss, N., Schubert, W.-D., Klukas, O., Fromme, P., Witt, H. T., and Saenger, W. (1996) *Nat. Struct. Biol. 3*, 965−973.
3. Kim, S.-T., Sancar, A., Essenmacher, C., and Babcock, G. T. (1993) *Proc. Natl. Acad. Sci. U.S.A. 90*, 8023−8027.
4. Harkins, T. T. and Grissom, C. B. (1994) *Science 263*, 958−960.
5. Salikhov, K. M., Kandrashkin, Y. E., and Salikhov, A. K. (1992) *Appl. Magn. Reson. 3*, 199−216.
6. Dzuba, S. A., Gast, P., and Hoff, A. J. (1995) *Chem. Phys. Lett. 236*, 595−602.
7. Zech, S. G., Lubitz, W., and Bittl, R. (1996) *Ber. Bunsen-Ges. Phys. Chem. 100*, 2041−2044.
8. Bittl, R., and Zech, S. G. (1997) *J. Phys. Chem. B 101*, 1429−1436.
9. Dzuba, S. A., Hara, H., Kawamori, A., Iwaki, M., Itoh, S., and Tsvetkov, Y. D. (1997) *Chem. Phys. Lett. 264*, 238−244.
10. Brettel, K., Sieckmann, I., van der Est, A., Fromme, P., and Stehlik, D. (1992) *Biochim. Biophys. Acta 1098*, 266−270.
11. Kamlowski, A., van der Est, A., Fromme, P., and Stehlik, D. (1997) *Biochim. Biophys. Acta 1319*, 185−198.
12. Käss, H., Fromme, P., Witt, H. T., and Lubitz, W. (1994) *Biophys. J. 66*, A228.
13. Käss, H. (1995) *Die Struktur des primären Donators $P_{700}$ in Photosystem I−Untersuchungen mit Methoden der stationären und gepulsten Elektronenspinresonanz*, Doctoral Thesis, Technische Universität Berlin.
14. Vallon, O., and Bogorad, L. (1993) *Eur. J. Biochem. 214*, 907−915.
15. van der Est, A., Prisner, T., Bittl, R., Fromme, P., Lubitz, W., Möbius, K., and Stehlik, D. (1997) *J. Phys. Chem. 101*, 1437−1443.
16. Iwaki, M., Kumazaki, S., Yoshita, K., Erabi, T., and Itoh, S. (1996) *J. Phys. Chem. 100*, 10802−10809.
17. Berry, M. C., Bratt, P. J., and Evans, M. C. W. (1997) *Biochim. Biophys. Acta 1319*, 163−176.
18. MacMillan, F., Hanley, J., van der Weerd, L., Knüpling, M., Un, S., and Rutherford, A. W. (1997) *Biochemistry 36*, 9297−9303.
19. Sétif, P., and Brettel, K. (1993) *Biochemistry 32*, 7846−7854.
20. Schlodder, E., Brettel, K., Falkenberg, K., and Gergeleit, M. (1995) in *Photosynthesis: from Light to Biosphere* (Mathis, P., Ed.) Vol. II, pp 107−110, Kluwer Academic Publishers, Boston.
21. Schubert, W.-D., Klukas, O., Krauss, N., Saenger, W., Fromme, P., and Witt, H. T. (1997) *J. Mol. Biol.* (in press).

BI971645N